Contribution from the Department of Chemistry,
Harvard University, Cambridge, Massachusetts 02138

Low-Potential Nickel(III,II) Complexes: New Systems Based on Tetradentate Amidate-Thiolate Ligands and the Influence of Ligand Structure on Potentials in Relation to the Nickel Site in [NiFe]-Hydrogenases

H.-J. Krüger, Gang Peng, and R. H. Holm*

Received July 25, 1990

In a continuing study of $Ni^{II,III}$ complexes with low redox potentials that are of possible relevance to the nickel site in [NiFe]-hydrogenases, Ni^{II} complexes of the tetraanions of the amide-thiol ligands *N,N'*-ethylenebis(2-mercaptoacetamide) (H_4ema), *N,N'*-1,2-phenylenebis(2-mercaptoacetamide) (H_4phma), and *N,N'*-ethylenebis(2-mercaptoisobutyramide) (H_4emi) have been prepared. The ligands were isolated as their *S*-acetyl derivatives; their reaction with Ni^{II} under basic conditions afforded the red diamagnetic complexes $[Ni(ema)]^{2-}$ (**5**), $[Ni(phma)]^{2-}$ (**6**), and $[Ni(emi)]^{2-}$ (**7**), which were isolated as Et_4N^+ salts. The tetradentate nature of the ligands was demonstrated by the X-ray structure determination of $(Et_4N)_2[Ni(ema)]\cdot 2H_2O$, which crystallizes in orthorhombic space group *Pnma* with a = 28.973 (8) Å, b = 12.239 (4) Å, c = 8.389 (2) Å, and Z = 4. The anion is planar with Ni-S = 2.179 (1) Å and Ni-N = 1.857 (3) Å. The complexes undergo reversible one-electron oxidations ($E_{1/2}$ vs SCE, cyclic voltammetry) in DMF solutions: $[Ni(ema)]^{-,2-}$, -0.34 V; $[Ni(phma)]^{-,2-}$, -0.24 V; $[Ni(emi)]^{-,2-}$, -0.42 V. The EPR spectra of the products demonstrate metal-centered oxidation to form Ni^{III} species; of these, $[Ni(emi)]^-$ is the most stable, but it could not be isolated in pure condition. These potentials are among the lowest known for the $Ni^{III,II}$ couple. The factors affording low potentials of this couple in complexes prepared in this and other laboratories are summarized. Chief among these are anionic polarizable ligands and 2- net charge of the Ni^{II} complexes. Electronic structural calculations were made for the low-potential complexes $[Ni(pdtc)_2]^{-,2-}$ (pdtc = pyridine-2,6-bis(thiocarboxylate)(2-)) and $[Ni(nbdt)_2]^{1-,2-}$ (nbdt = norbornane-2,3-dithiolate(2-)); for the respective Ni^{III} species the ground states $\sigma^*(d_{z^2})$ and $\pi^*(d_{xz}$ or $d_{yz})$ are indicated. When nominally compared, the $[Ni(emi)]^{-,2-}$ potential is close to that (-0.39 V) for reduction of the Ni-A state in *Desulfovibrio gigas* hydrogenase. However, when the effects of solvent and pH on redox potentials are considered, it is concluded that, among synthetic species, the potential of the $[Ni(nbdt)_2]^{-,2-}$ couple is closest to that of the enzyme site. Cysteinate is likely the most effective native ligand in stabilizing Ni^{III}, but not all biological modes of metal ligation may have been discovered.

Introduction

One of the many highly unusual and unexplained electronic and reactivity features of [NiFe]-hydrogenases[1-3] is the low values of their Ni^{III}/Ni^{II} redox potentials. Of these enzymes, *Desulfovibrio gigas* hydrogenase has been examined in considerable detail.[2-5] It has been obtained in two fully oxidized forms, "unready" and "ready", which contain the EPR-distinguishable states Ni-A (g = 2.31, 2.23, 2.02) and Ni-B (g = 2.33, 2.16, 2.02), respectively. For Ni-A, E_m = -0.39 V vs SCE at pH 7 with a dependence of -60 mV/pH unit.[4,6] This value is substantially more negative than those of the large majority of Ni^{III}/Ni^{II} potentials of synthetic complexes.[7] Current evidence suggests that the Ni^{III}-B state is the entrance point to the catalytic cycle of the enzyme.[6]

The marked relative stability of Ni^{III} in states Ni-A and Ni-B must derive from the stereochemistry and ligation mode of the coordination unit, together with any beneficial influences of protein folding and environment. This situation is modulated by the effect of an acid-base equilibrium, as reflected in the pH dependence of the potentials. We have adopted the premise that elucidation of factors that lead to the stabilization of Ni^{III} could afford structural and electronic information regarding the stabilization of this oxidation state in enzyme sites. Accordingly, we have investigated the redox chemistry of a series of Ni complexes with the intention of achieving reversible reactions with relatively low potentials. Most of these complexes contain in part (anionic) sulfur ligands, a feature indicated by EXAFS results for the oxidized enzymes from *D. gigas* and *Methanobacterium thermoautotrophicum*.[8] Certain Ni^{II} complexes of this type undergo electrochemically[9,10] or chemically[11] induced reactions of undesirable ligand-based oxidation. Others sustain metal-centered oxidation to afford products that are meaningfully formulated as Ni^{III} complexes.[12-14] In recent work, we utilized EPR and structural criteria for the purpose of establishing the Ni^{III} formulation.[13]

Depicted in Figure 1 are four types of complexes **1-4** examined in this laboratory[12,13] which display chemically reversible $Ni^{III,II}$ redox couples with half-wave potentials $E_{1/2}$ between +0.13 and -0.74 V in DMF solutions. In all cases, the oxidized complexes were sufficiently stable for detection by EPR spectroscopy, and in addition, $[Ni(pdtc)_2]^-$ (**3**) was isolated and structurally characterized. The most conspicuous features of **1-4** are planar or tetragonal stereochemistry and the presence of four polarizable anionic ligands, features evidently congenial to the stabilization

(1) Cammack, R. *Adv. Inorg. Chem.* **1988**, *32*, 297.
(2) Cammack, R.; Fernandez, V. M.; Schneider, K. In *The Bioinorganic Chemistry of Nickel*; Lancaster, J. R., Jr., Ed.; VCH Publishers, Inc.: New York, 1988; Chapter 8.
(3) Moura, J. J. G.; Teixeira, M.; Moura, I.; LeGall, J. In *The Bioinorganic Chemistry of Nickel*; Lancaster, J. R., Jr., Ed.; VCH Publishers, Inc.: New York, 1988; Chapter 9.
(4) (a) Cammack, R.; Patil, D.; Aguirre, R.; Hatchikian, E. C. *FEBS Lett.* **1982**, *142*, 289. (b) Teixeira, M.; Moura, I.; Xavier, A. V.; DerVartanian, D. V.; LeGall, J.; Peck, H. D., Jr.; Huynh, B. H. *Eur. J. Biochem.* **1983**, *130*, 481.
(5) (a) Teixeira, M.; Moura, I.; Xavier, A. V.; Huynh, B. H.; DerVartanian, D. V.; Peck, H. D., Jr.; LeGall, J.; Moura, J. J. G. *J. Biol. Chem.* **1985**, *260*, 8942. (b) Cammack, R.; Patil, D.; Hatchikian, E. C.; Fernandez, V. M. *Biochim. Biophys. Acta* **1987**, *912*, 98. (c) Huynh, B. H.; Patil, D. S.; Moura, I.; Teixeira, M.; Moura, J. J. G.; DerVartanian, D. V.; Czechowski, M. H.; Prickril, B. C.; Peck, H. D., Jr.; LeGall, J. *J. Biol. Chem.* **1987**, *262*, 795. (d) Teixeira, M.; Moura, I.; Xavier, A. V.; Moura, J. J. G.; LeGall, J.; DerVartanian, D. V.; Peck, H. D., Jr.; Huynh, B. H. *J. Biol. Chem.* **1989**, *264*, 16435.
(6) Upon reduction, the ready form is activated rapidly and unready form is activated slowly, possibly due to the necessity of a protein conformational change of the latter form. The Ni-B potential has not been accurately measured; a current estimate places it at a value slightly more negative than -150 mV.[5d]
(7) (a) Nag, K.; Chakravorty, A. *Coord. Chem. Rev.* **1980**, *33*, 87. (b) Haines, R. J.; McAuley, A. *Coord. Chem. Rev.* **1981**, *39*, 77. (c) Lappin, A. G.; McAuley, A. *Adv. Inorg. Chem.* **1988**, *32*, 241.
(8) (a) Lindahl, P. A.; Kojima, N.; Hausinger, R. P.; Fox, J. A.; Teo, B.-K.; Walsh, C. T.; Orme-Johnson, W. H. *J. Am. Chem. Soc.* **1984**, *106*, 3062. (b) Scott, R. A.; Wallin, S. A.; Czechowski, M.; DerVartanian, D. V.; LeGall, J.; Peck, H. D., Jr.; Moura, I. *J. Am. Chem. Soc.* **1984**, *106*, 6864. (c) Scott, R. A.; Czechowski, M.; DerVartanian, D. V.; LeGall, J.; Peck, H. D., Jr.; Moura, I. *Rev. Port. Quim.* **1985**, *27*, 67.
(9) Nakabayashi, Y.; Matsuda, Y.; Sekido, E. *J. Electroanal. Chem. Interfacial Electrochem.* **1986**, *205*, 209.
(10) Krüger, H.-J.; Holm, R. H. *Inorg. Chem.* **1989**, *28*, 1148.
(11) (a) Kumar, M.; Day, R. O.; Colpas, G. J.; Maroney, M. J. *J. Am. Chem. Soc.* **1989**, *111*, 5974. (b) Kumar, M.; Colpas, G. J.; Day, R. O.; Maroney, M. J. *J. Am. Chem. Soc.* **1989**, *111*, 8323.
(12) Krüger, H.-J.; Holm, R. H. *Inorg. Chem.* **1987**, *26*, 3645.
(13) Krüger, H.-J.; Holm, R. H. *J. Am. Chem. Soc.* **1990**, *112*, 2955.
(14) Fox, S.; Wang, Y.; Silver, A.; Millar, M. *J. Am. Chem. Soc.* **1990**, *112*, 3218.

0020-1669/91/1330-0734$02.50/0

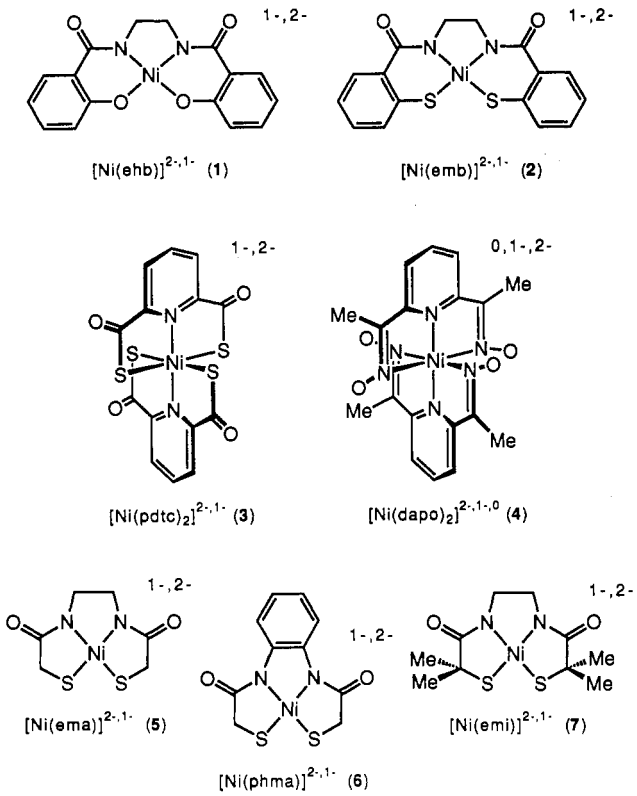

Figure 1. Structural formulas of $Ni^{II,III}$ complexes **1–7** and their abbreviations. Complexes **1**/**2**[12] and **3**/**4**[13] have been examined previously; complexes **5–7** are the subjects of this investigation.

of Ni^{III}. Ligand groups include phenolate, thiolate, thiocarboxylate, oximate, and amidate; all are of conceivable physiological occurrence but only the first two have been proven in metalloproteins.[15] In any attempt to establish a more general basis for achievement of the Ni^{III} state, account should be taken of the comprehensive studies of Margerum and co-workers,[16] who have demonstrated the value of deprotonated peptides (amidates) for the stabilization of Ni^{III}. Amidate groups have also been incorporated into cyclic tetra- and pentaaza ligands with a similar effect.[17,18] The Ni^{III} complexes of peptide and tetraaza ligands are usually too unstable to be isolated. However, in one case, the Ni^{II} and Ni^{III} complexes of the same pentaaza ligand have been isolated and structurally characterized.[19] While otherwise of considerable interest, such complexes do not possess low potentials. An indication that thiol-containing peptides could form trivalent nickel complexes was afforded by the work of Sugiura et al.[20a,b] and Mascharak and co-workers.[20c] However, no complexes were isolated and potentials, where measured, were not unusual. Nonetheless, these findings, when taken together with the properties of **2** ($E_{1/2}$ = −0.04 V) suggested that amidate–thiolate ligation might be an effective means of stabilizing low-potential Ni^{III}. No Ni^{II} complex with this type of ligation, other than $[Ni(emb)]^{2-}$ (**2**), had been isolated. We report here our study of three new amidate–thiolate complexes **5–7** (Figure 1) together with considerations of the electronic structures and other aspects of low-potential $Ni^{III,II}$ complexes prepared in this laboratory and elsewhere.

Experimental Section

Preparation of Compounds. (1) Ligands. Reagents used in the following preparations were commercial samples.

***N,N'*-Ethylenebis(2-(acetylthio)acetamide) (8). (a) *N,N'*-Ethylenebis(2-chloroacetamide).** Ethylenediamine (10.0 mL, 150 mmol) in 40 mL of chloroform and pyridine (24.0 mL, 297 mmol) were successively added dropwise to an ice-cold solution of 24.0 mL (301 mmol) of chloroacetyl chloride in 300 mL of chloroform. The reaction mixture was warmed to room temperature and stirred for 12 h. The solid resulting from removal of the solvent in vacuo was treated with water, and the mixture was filtered. The collected material was washed thoroughly with water and with a small amount of ether to afford 13.6 g (43%) of a white solid. ^1H NMR (Me_2SO-d_6): δ 3.16 (dd, 4), 4.03 (s, 4), 8.26 (br, 2).

(b) Compound 8. A slurry of 13.6 g (64 mmol) of the preceding compound in 200 mL of ethanol was combined with 100 mL of a methanolic solution containing 8.60 g (153 mmol) of KOH and 12.0 mL (168 mmol) of thiolacetic acid. The reaction mixture was refluxed for 3 h and stirred at room temperature for 12 h. The precipitate was collected by filtration and washed with copious amounts of water. Recrystallization from ethanol led to 18.3 g (98%) of product as slightly yellow crystalline flakes, mp 159–160 °C. Anal. Calcd for $C_{10}H_{16}N_2O_4S_2$: C, 41.08; H, 5.52; N, 9.58. Found: C, 41.03; H, 5.44; N, 9.44. FAB-MS (3-nitrobenzyl alcohol): 293 ($M + H^+$). ^1H NMR ($CDCl_3$): δ 2.43 (s, 6), 3.37 (dd, 4), 3.54 (s, 4), 6.67 (br, 2). IR (KBr): 3308, 1687, 1647, 1537, 1447, 1378, 1332, 1240, 1139, 635 cm^{-1} (strong bands only).

***N,N'*-1,2-Phenylenebis(2-(acetylthio)acetamide) (9). (a) *N,N'*-1,2-Phenylenebis(2-chloroacetamide).** An analogous procedure was followed to obtain 27.8 g (71%) of product from 16.2 g (150 mmol) of 1,2-phenylenediamine in 100 mL of THF and 24.0 mL (301 mmol) of chloroacetyl chloride in chloroform. ^1H NMR (Me_2SO-d_6): δ 4.31 (s, 4), 7.21 (dd, 2), 7.52 (dd, 2), 9.68 (br, 2).

(b) Compound 9. A slurry of 27.8 g (106 mmol) of the preceding compound in 200 mL of ethanol was combined with 100 mL of a methanolic solution of 13.4 g (239 mmol) of KOH and 19.0 mL (266 mmol) of thiolacetic acid. The mixture was refluxed for 3 h and was colled to room temperature. The solid was collected by filtration and extensively washed with water. The filtrate was reduced in volume to yield a second crop of solid, which was collected and thoroughly washed with water. The combined crops were recrystallized from ethanol to afford 28.2 g (78%) of product as white needles, mp 127 °C. Anal. Calcd for $C_{14}H_{16}N_2O_4S_2$: C, 49.39; H, 4.74; N, 8.23. Found: C, 49.40; H, 4.68; N, 8.10. FAB-MS (3-nitrobenzyl alcohol): 341 ($M + H^+$). ^1H NMR ($CDCl_3$): δ 2.46 (s, 6), 3.74 (s, 4), 7.20 (dd, 2), 7.48 (dd, 2), 8.34 (br, 2). IR (KBr): 3236, 1699, 1666, 1542, 1455, 1328, 1134, 627 cm^{-1} (strong bands only).

***N,N'*-Ethylenebis(2-(acetylthio)isobutyramide) (10). (a) *N,N'*-Ethylenebis(2-bromoisobutyramide).** An analogous procedure gave 43.7 g (82%) of product from 10.0 mL (150 mmol) of ethylenediamine and 37.0 mL (299 mmol) of 2-bromoisobutyryl bromide. ^1H NMR (Me_2SO-d_6): δ 1.96 (s, 12), 3.48 (dd, 4), 7.16 (br, 2).

(b) *N,N'*-Ethylenebis(2-(benzylthio)isobutyramide). The preceding compound (43.7 g, 122 mmol) was added to a solution prepared from 27.0 g (481 mmol) of KOH and 57.0 mL (486 mmol) of phenylmethanethiol in 200 mL of ethanol. The reaction mixture was refluxed for 6 h, cooled to room temperature, and diluted 4-fold with water. The white solid that separated was collected by filtration and thoroughly washed with water and a small amount of ether to afford 50.9 g (94%) of product. ^1H NMR ($CDCl_3$): δ 1.53 (s, 12), 3.19 (dd, 4), 3.73 (s, 4), 6.04 (br), 7.22–7.32 (m, 10).

(c) Compound 10. To a suspension of 50.9 g (114 mmol) of the preceding compound in liquid ammonia was added a total of 12.3 g of sodium metal in small portions until the blue color persisted for at least 15 min. The solution was stirred for another 30 min, and the excess reducing equivalents were destroyed by addition of NH_4Cl. The ammonia was evaporated, and the solid residue was dissolved in methanol under anaerobic conditions. The solution was cooled to 0 °C, 100 mL

(15) The presence of selenocysteinate as a ligand on Ni in *Desulfovibrio baculatus* [NiFeSe]-hydrogenase provides a further reminder of the possibility of unconventional (or at least unexpected) binding modes in metalloproteins: (a) Eidsness, M. K.; Scott, R. A.; Prickril, B. C.; DerVartanian, D. V.; LeGall, J.; Moura, I.; Moura, J. J. G.; Peck, H. D., Jr. *Proc. Natl. Acad. Sci. U.S.A.* **1989**, *86*, 147. (b) He, S. H.; Teixeira, M.; LeGall, J.; Patil, D. S.; Moura, I.; Moura, J. J. G.; DerVartanian, D. V.; Huynh, B. H.; Peck, H. D., Jr. *J. Biol. Chem.* **1989**, *264*, 2678.

(16) (a) Bossu, F. P.; Margerum, D. W. *Inorg. Chem.* **1977**, *16*, 1210. (b) Bossu, F. P.; Paniago, E. B.; Margerum, D. W.; Kirksey, S. T., Jr.; Kurtz, J. L. *Inorg. Chem.* **1978**, *17*, 1034. (c) Lappin, A. G.; Murray, C. K.; Margerum, D. W. *Inorg. Chem.* **1978**, *17*, 1630. (d) Youngblood, M. P.; Margerum, D. W. *Inorg. Chem.* **1980**, *19*, 3068. (e) Murray, C. K.; Margerum, D. W. *Inorg. Chem.* **1982**, *21*, 3501. (f) Subak, E. J., Jr.; Loyola, V. M.; Margerum, D. W. *Inorg. Chem.* **1985**, *24*, 4350. (g) Kirvan, G. E.; Margerum, D. W. *Inorg. Chem.* **1985**, *24*, 3245. (h) Wang, J.-F.; Kumar, K.; Margerum, D. W. *Inorg. Chem.* **1989**, *28*, 3481.

(17) Kimura, E. *Coord. Chem. Rev.* **1986**, *15*, 1.

(18) Sigel, H.; Martin, R. B. *Chem. Rev.* **1982**, *82*, 385.

(19) Machida, R.; Kimura, E.; Kushi, Y. *Inorg. Chem.* **1986**, *25*, 3461.

(20) (a) Sugiura, Y.; Mino, Y. *Inorg. Chem.* **1979**, *18*, 1336. (b) Sugiura, Y.; Kuwahara, J.; Suzuki, T. *Biochem. Biophys. Res. Commun.* **1983**, *115*, 878. (c) Baidya, N.; Olmstead, M. M.; Mascharak, P. K. *Inorg. Chem.* **1989**, *28*, 3426.

Table I. Crystallographic Data for $(Et_4N)_2[Ni(ema)]\cdot 2H_2O$

formula	$C_{22}H_{52}N_4NiO_4S_2$	V, Å^3	2975 (2)
fw	559.50	T, K	298
space group	*Pnma*	ρ_{calcd} (ρ_{obs}), g/cm^3	1.25 (1.25)[a]
a, Å	28.973 (8)	abs coeff, μ, cm^{-1}	8.19
b, Å	12.239 (4)	$R(F_o)$, %	4.75
c, Å	8.389 (2)	$R_w(F_o^2)$, %	5.64
Z	4		

[a] Determined by neutral buoyancy in CCl_4/hexane.

of acetic anhydride was added, the mixture was stirred for 2 h, and it was treated with 400 mL of water. A small amount of white solid was removed by filtration, and the filtrate was reduced in vacuo to a solid residue. Addition of water to the residue followed by agitation of the mixture caused separation of a white precipitate, which was collected by filtration and successively washed with water and small amounts of ether. The product (21.4 g, 54%) was isolated as a white solid. An analytical sample was obtained by recrystallization from ethyl acetate/hexane; mp 120–121 °C. Anal. Calcd for $C_{14}H_{24}N_2O_4S_2$: C, 48.25; H, 6.94; N, 8.04. Found: C, 48.65; H, 7.15; N, 7.92. FAB-MS (3-nitrobenzyl alcohol): 349 ($M + H^+$). ^1H NMR ($CDCl_3$): δ 1.61 (s, 12), 2.29 (s, 6), 3.37 (dd, 4), 7.14 (br, 2). IR (KBr): 3300, 1683, 1634, 1548, 1360, 1287, 1108, 633 cm^{-1} (strong bands only).

(2) Nickel(II) Complexes. Preparations were carried out under a pure dinitrogen atmosphere.

$(Et_4N)_2[Ni(ema)]$ ($(Et_4N)_2$[5]). A solution of 1.61 g (5.51 mmol) of **8**, 1.54 g (27.4 mmol) of KOH, and 1.65 g (10.0 mmol) of Et_4NCl in 75 mL of methanol was stirred for 30 min. A solution of 1.24 g (4.98 mmol) of $Ni(OAc)_2\cdot 4H_2O$ in 40 mL of methanol was added dropwise, generating a red solution. After being stirred for 15 min, the solution was taken to dryness in vacuo, and the solid residue was treated with acetonitrile. The resultant red solution was filtered, the volume of the filtrate was reduced to 20 mL, and this solution was filtered. Ether was diffused into the solution, causing the separation of red crystals. These were collected, washed with 1:1 MeCN/ether (v/v), and purified by two cycles of ether diffusion into acetonitrile solutions of the compound. This procedure afforded 1.38 g (53%) of pure product as dark red crystals. Anal. Calcd for $C_{22}H_{48}N_4NiO_2S_2$: C, 50.48; H, 9.24; N, 10.70; Ni, 11.22; S, 12.25. Found: C, 50.38; H, 9.35; N, 10.36; Ni, 11.09; S, 12.23. ^1H NMR (CD_3CN, anion): δ 2.65 (s, 4), 2.80 (s, 4). Absorption spectrum (EtOH): λ_{max} (ϵ_M) 261 (22 500), 437 (405), 552 nm (79).

$(Et_4N)_2[Ni(phma)]$ ($(Et_4N)_2$[6]). This compound was prepared on the same scale by the above procedure with use of **9**. Slow diffusion of ether into the red solution obtained from acetonitrile treatment of the solid residue gave red crystals, which were isolated and washed with 1:1 MeCN/ether (v/v). This material was recrystallized by slow diffusion of ether into an acetonitrile solution. After the collected solid was washed with MeCN/ether and ether, the produce was obtained as 1.99 g (70%) of dark red crystals. Anal. Calcd for $C_{25}H_{48}N_4NiO_2S_2$: C, 54.64; H, 8.47; N, 9.80; Ni, 10.27; S, 11.22. Found: C, 54.75; H, 8.50; N, 9.50; Ni, 10.16; S, 11.50. ^1H NMR (CD_3CN, anion): δ 2.87 (s, 4), 6.51 (dd, 2), 8.53 (dd, 2). Absorption spectrum (EtOH): λ_{max} (ϵ_M) 261 (sh, 25 200), 334 (7180), 443 (289), 556 nm (88).

$(Et_4N)_2[Ni(emi)]\cdot 2H_2O$ ($(Et_4N)_2$[7]$\cdot 2H_2O$). This compound was prepared on the same scale by the above procedure with use of **10**. Workup as for **6** afforded the pure product as 1.08 g (35%) of red needles. Anal. Calcd for $C_{26}H_{60}N_4NiO_4S_2$: C, 50.72; H, 9.82; N, 9.10; Ni, 9.54; S, 10.42. Found: C, 51.02; H, 10.04; N, 9.37; Ni, 9.42; S, 10.90. ^1H NMR (CD_3CN, anion + H_2O): δ 1.14 (s, 12), 2.59 (s, 4), 2.81 (s, 4). Absorption spectrum (EtOH): λ_{max} (ϵ_M) 261 (23 600), 430 (340), 534 nm (79).

Collection and Reduction of X-ray Data. A suitable single crystal of $(Et_4N)_2[Ni(ema)]\cdot 2H_2O$ was cut from a larger needle obtained during the first slow ether diffusion as described in the previous section. The crystal was mounted in a sealed glass capillary under a dinitrogen atmosphere. Data collection was carried out at ambient temperature on a Siemens R3m/V automated four-circle diffractometer using graphite-monochromatized Mo Kα radiation. Crystallographic data are listed in Table I. The unit cell parameters and the final orientation matrices were obtained from least-squares refinement of machine-centered reflections. Intensities of three standard reflections monitored every 47 reflections indicated no decay of the crystal during data collection. The data sets were processed with the program XTAPE of the SHELXTL program package (Nicolet XRD Corp., Madison, WI). Semiempirical absorption corrections were applied by using the program XEMP. The systematic absences $0kl$ ($l = 2n + 1$), $hk0$ ($h + k = 2n + 1$), $h00$ ($h = 2n + 1$), $0k0$ ($k = 2n + 1$), and $00l$ ($l = 2n + 1$) are consistent with the unconventional orthorhombic space groups $Pc2_1n$ (No. 33) and *Pcmn* (No. 62). The data output were therefore converted to the conventional space groups $Pc2_1a$ (No. 33) and *Pnma* (No. 62), in which the systematic absences are $0kl$ ($k + l = 2n + 1$), $hk0$ ($h = 2n + 1$), $h00$ ($h = 2n + 1$), $0k0$ ($k = 2n + 1$), and $00l$ ($l = 2n + 1$). Simple E statistics favored the centrosymmetric space group *Pnma*. Subsequent successful solution and refinement of the structure proved this choice to be correct.

Table II. Positional Parameters ($\times 10^4$) for the Non-Hydrogen Atoms and Located Hydrogen Atoms of $(Et_4N)_2[Ni(ema)]\cdot 2H_2O$

atom	x/a	y/b	z/c
Ni(1)	1144.5 (3)	2500	2062 (1)
S(1)	1041.0 (4)	1162 (1)	387 (1)
N(1)	1225 (1)	1469 (3)	3663 (4)
O(1)	1266 (1)	−309 (2)	4529 (4)
C(1)	1126 (2)	39 (4)	1762 (6)
C(2)	1211 (2)	403 (4)	3466 (5)
C(3)	1305 (2)	1888 (4)	5266 (6)
N(2)	2609 (2)	2500	9630 (6)
C(4)	2783 (3)	2500	11325 (9)
C(5)	2391 (4)	2500	12565 (10)
C(6)	3041 (2)	2500	8602 (10)
C(7)	2971 (4)	2500	6830 (11)
C(8)	2313 (2)	3488 (4)	9288 (6)
C(9)	2536 (2)	4589 (4)	9622 (7)
N(3)	4659 (2)	2500	2167 (6)
C(10)	4413 (3)	2500	3751 (9)
C(11)	4742 (4)	2500	5176 (11)
C(12)	4265 (3)	2500	927 (11)
C(13)	4442 (3)	2500	−731 (10)
C(14)	4968 (2)	3507 (4)	2043 (7)
C(15)	4728 (2)	4581 (4)	2131 (8)
O(2)	3460 (1)	444 (3)	2689 (4)
H(27)	3535	−160	3321
H(28)	3576	337	1690

Structure Solution and Refinement. The nickel atom was located by a Patterson map; the remaining non-hydrogen atoms were found by means of Fourier difference maps between the observed and calculated structure factors by using the program CRYSTALS. Atomic scattering factors were taken from a standard source.[21] Isotropic refinement converged at 10.5%. The nickel atom of the complex and the nitrogen atoms and four carbon atoms of both cations are located on a special position of a mirror plane (x, 0.25, y). Therefore, during refinement the y positions of these atoms were fixed and the anisotropic temperature factors $U(12)$ and $U(23)$ were set to zero. All non-hydrogen atoms were described anisotropically. The hydrogen atoms of the water molecule were located by a Fourier difference map. In the final stages of the refinement, the ligand hydrogen atoms were introduced at 0.98 Å from the bonded carbon with isotropic thermal parameters of 0.1 Å^2. Four reflections (hkl: 15,2,1; 5,11,2; 21,2,3; 22,0,5) were omitted in the refinement, since their calculated structure factors deviate by more than 20σ from the observed ones. These erroneous reflections were probably caused by some slight twinning. A final difference Fourier map revealed no peaks larger than 0.56 e/Å^3. The final R factors are given in Table I. Positional parameters are collected in Table II.[22]

Other Physical Measurements. Fast atom bombardment (FAB) mass spectra were obtained with a Kratos MS-50 mass spectrometer. Absorption spectra were recorded on Varian 2390 and Perkin-Elmer Lambda 4C spectrophotometers. NMR spectra were taken on a Bruker AM-250 NMR spectrometer. Infrared spectra were recorded on a Nicolet FT-IR 43 instrument. EPR spectra were obtained with a Varian E Line Century spectrometer operating at X-band frequencies. Solutions of the electrochemically generated complexes were frozen in liquid nitrogen prior to recording the EPR spectra. Electrochemical experiments were carried out on a PAR M-370 system placed in an inert-atmosphere box. Low-tempertaure experiments were performed by immersing an electrochemical cell, specially equipped with ground-glass joints for anaerobic work, into an acetone/dry ice bath. In cyclic voltammetry, 1 mM solutions of complexes in DMF containing 0.2 M $(Bu_4N)ClO_4$ supporting electrolyte were used. All potentials were measured vs a SCE reference electrode at 25 °C; no corrections were made for junction potentials. A Pt-foil electrode was employed as the working electrode. Under these conditions, the potential for the $[(C_5H_5)_2Fe]^{+,0}$ couple was 0.48 V. Coulometric experiments were performed with use of a Pt-gauze electrode and a PAR Model 173 potentiostat equipped with a PAR Model 179 digital coulometer.

(21) Cromer, D. T.; Waber, J. T. *International Tables for X-Ray Crystallography*; Kynoch Press: Birmingham, England, 1974.

(22) See paragraph at end of paper concerning supplementary material.

Computational Details. Molecular orbital calculations on $Ni^{II,III}$ and Co^{III} complexes were performed by the Fenske–Hall nonempirical approximate method[23] on a MicroVAX II. The usual Ni and Co wave functions were used, with coefficients 0.5959, 0.5497, and exponents 5.75, 2.40 for Ni and coefficients 0.5680, 0.6060 and exponents 5.55, 2.10 for Co. Molecular geometries were taken from X-ray crystallographic results obtained in previous work.[13,14]

Results and Discussion

Ligand Preparations. The synthesis of *N,N'*-ethylenebis(2-mercaptoacetamide) from methyl 2-mercaptoacetate and ethylenediamine has been reported.[24] The route is sometimes accompanied by side reactions and low yields. Here we first prepared the corresponding bis(2-chloroacetamide) and converted it with thioacetate to the bis(2-(acetylthio)acetamide) (**8**). Compound **9** was prepared analogously; a similar means has been utilized in the preparation of the dibenzoyl variants of **8** and **9**.[25] The protected ligands rather than the free thiols were prepared because of easier purification and long-term storage without decomposition. The same method could not be applied to **10** because of thioacetate. difficulty of displacing halide from a tertiary carbon atom with thioacetate. Reaction sequence 1 was adopted, in which

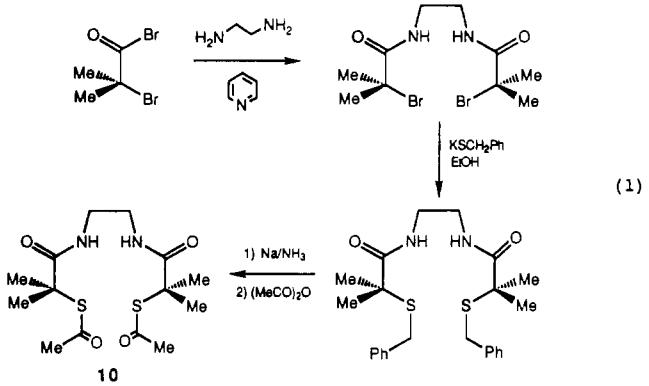

(1)

10

bromide was displaced from the dibromo intermediate with phenylmethanethiolate in 94% yield. The *S*-benzyl groups were cleaved to yield the dithiolate anion, which was acetylated to afford **10** in 54% yield (42% overall yield from the acyl dibromide).

Ni(II) Complexes. The syntheses of $[Ni(ema)]^{2-}$ (**5**), $[Ni(phma)]^{2-}$ (**6**), and $[Ni(emi)]^{2-}$ (**7**) were implemented by ligand deprotection in basic methanol, followed by addition of $Ni(OAc)_2$ and isolation as Et_4N^+ salts. The compounds are diamagnetic and exhibit the absorption spectra in Figure 2, in which sets of d–d bands are observed at 534–556 and 430–443 nm in ethanol. For $[Ni(emb)]^{2-}$[12] in ethanol, the first d–d band occurs at 581 nm. The apparently corresponding d–d bands in the planar bis(dithiolate) complexes **11**[26] (635, 482 nm) and $[\mathbf{12}]^{2-}$[14] (633,

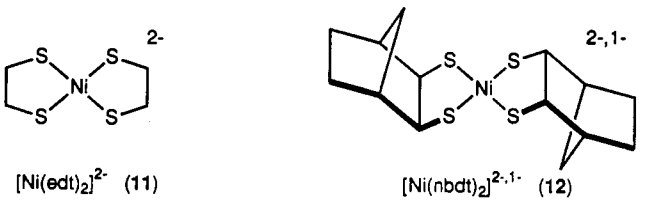

$[Ni(edt)_2]^{2-}$ (**11**) $[Ni(nbdt)_2]^{2-,1-}$ (**12**)

460 nm) are found at lower energies, indicating that the combination of two thiolate and two amidate ligands exerts a stronger in-plane ligand field. All compounds are quite soluble in protic and dipolar aprotic solvents. It is noteworthy that protic solvents do not induce oligomerization, which is common to Ni^{II} thiolates.[26-28] In contrast to $[\mathbf{2}]^{2-}$, nickel(II) complexes **5**–**7** are

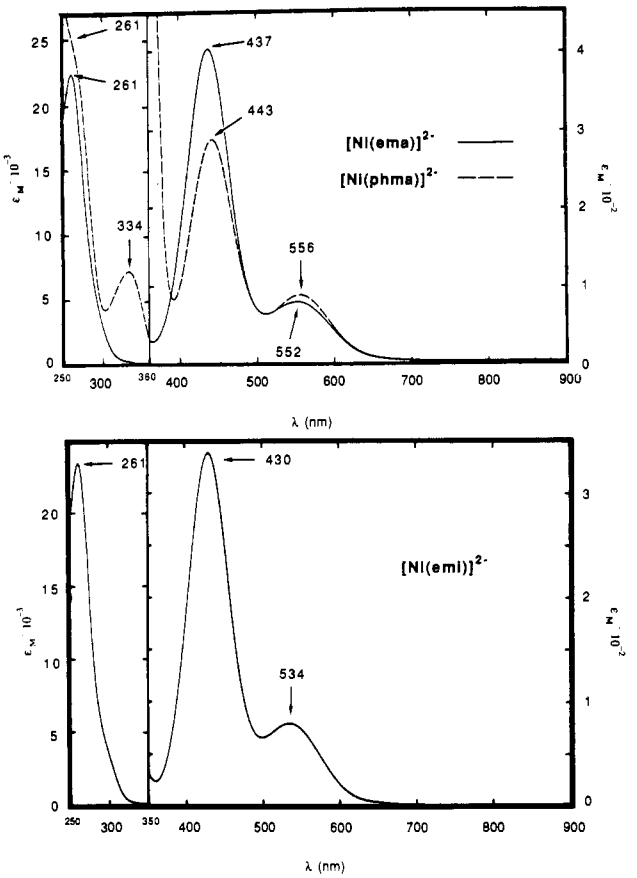

Figure 2. Electronic absorption spectra of $[Ni(ema)]^{2-}$ and $[Ni(phma)]^{2-}$ (upper) and $[Ni(emi)]^{2-}$ (lower) in ethanol solutions. Band maxima are indicated.

Table III. Selected Interatomic Distances (Å) and Angles (deg) for $(Et_4N)_2[Ni(ema)]\cdot 2H_2O$

Ni(1)–S(1)	2.179 (1)	Ni(1)–N(1)	1.857 (3)
S(1)–C(1)	1.811 (5)	N(1)–C(2)	1.315 (3)
N(1)–C(3)	1.458 (6)	O(1)–C(2)	1.257 (5)
C(1)–C(2)	1.518 (6)	C(3)–C(3′)	1.499 (10)
S(1)–Ni(1)–S(1′)	97.44 (8)	N(1)–Ni(1)–S(1)	88.4 (1)
N(1)–Ni(1)–S(1′)	173.9 (1)	N(1)–Ni(1)–N(1′)	85.6 (2)
C(1)–S(1)–Ni(1)	98.1 (2)	C(2)–N(1)–Ni(1)	125.4 (3)
C(3)–N(1)–Ni(1)	116.6 (3)	C(3)–N(1)–C(2)	118.0 (4)
C(2)–C(1)–S(1)	113.5 (3)	O(1)–C(2)–N(1)	126.5 (4)
C(1)–C(2)–N(1)	114.5 (4)	C(1)–C(2)–O(1)	119.0 (4)
N(1)–C(3)–C(3′)	110.6 (2)		

sensitive to dioxygen and must be handled accordingly.

Structure of $[Ni(ema)]^{2-}$. The structure of this complex as its Et_4N^+ salt dihydrate is depicted in Figure 3. Selected metric parameters are contained in Table III. The complex is planar, with maximum deviations of ±0.022 Å from the least-squares plane, and has an imposed mirror plane perpendicular to the molecular plane and bisecting the C(3)–C(3′) bond. The complexes are linked by O–H···O and O–H···S hydrogen bonds to form infinite sheets. The pattern of three fused five-membered chelate rings imposes some steric strain. The ethylene bridge presents an eclipsed conformation of hydrogen atoms, and the N(1)–Ni–N(1′) angle is 85.6°. The rather tight fit on the NiN_2 side of the molecule causes an opening of the S(1)–Ni–S(1′) angle to 97.4°. This is a usual feature of planar complexes with the 5–5–5 ring pattern; three of the bond angles at the metal are roughly equal, and the fourth, less constrained, angle is appreciably larger.[29] The

(23) Fenske, R. F.; Hall, M. B. *Inorg. Chem.* **1972**, *11*, 768.
(24) Atkinson, E. R.; Handrick, G. R.; Bruni, R. J.; Granchelli, F. E. *J. Med. Chem.* **1965**, *8*, 29.
(25) Davison, A.; Jones, A. G.; Orvig, C.; Sohn, M. *Inorg. Chem.* **1981**, *20*, 1629.
(26) Snyder, B. S.; Rao, Ch. P.; Holm, R. H. *Aust. J. Chem.* **1986**, *39*, 963.
(27) Dance, I. G. *Polyhedron* **1986**, *5*, 1037.
(28) Tremel, W.; Kriege, M.; Krebs, B.; Henkel, G. *Inorg. Chem.* **1988**, *27*, 3886 and references therein.
(29) (a) Mulqi, M.; Stephens, F. S.; Vagg, R. S. *Inorg. Chim. Acta* **1981**, *52*, 73. (b) Stephens, F. S.; Vagg, R. S. *Inorg. Chim. Acta* **1982**, *57*, 9; **1986**, *120*, 165. (c) Freeman, H. C.; Guss, J. M.; Sinclair, R. L. *Acta Crystallogr.* **1978**, *B34*, 2459.

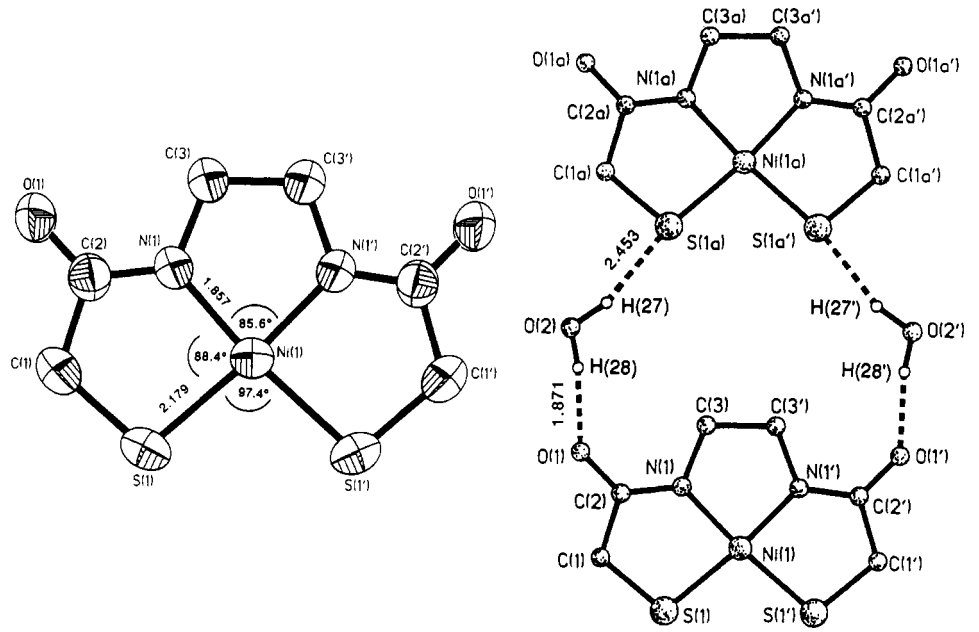

Figure 3. Structure of $[Ni(ema)]^{2-}$ showing 50% probability ellipsoids and the atom-labeling scheme (left) and the hydrogen-bonding interactions between two complexes (right). Several bond distances (Å) and angles are indicated.

Table IV. Comparative Properties of Low-Potential Ni(III) Complexes

complex	$E_{1/2}$, V[a]	g values[b]	ground state	stability	py adduct ($a_{\parallel}^{N}$, G)
$[Ni(ehb)]^-$ (**1**)[c]	+0.13	2.30, 2.10, 2.01	*h*	low	2:1 (19)
$[Ni(emb)]^-$ (**2**)[c]	−0.04	2.29, 2.11, 2.04	*h*	low	1:1 (21)
$[Ni(ema)]^-$ (**5**)	−0.34	2.23, 2.18, 2.01	$\sigma^*(d_{z^2})$	low	none
$[Ni(phma)]^-$ (**6**)	−0.24	2.20, 2.17, 2.01	$\sigma^*(d_{z^2})$	low	none
$[Ni(emi)]^-$ (**7**)	−0.42	2.44, 2.27, 1.96	*h*	high	1:1 (23)
$[Ni(nbdt)_2]^-$ (**12**)[d]	−0.76	2.14, 2.05	π^* (?)	?[f]	none
$[Ni(pdtc)_2]^-$ (**3**)[e]	−0.09	2.14, 2.04	$\sigma^*(d_{z^2})$	high	... (21)
$[Ni(dapo)_2]^-$ (**4**)[e]	−0.74	2.09[g]	*h*	low	... (≈25)

[a] Vs SCE; DMF; 25 °C. [b] DMF; 77–100 K; 25 K for **7**. [c] Reference 12. [d] Reference 14. [e] Reference 13. [f] Not reported; Ni^{III} complex not isolated. [g] g_{av}; poorly resolved spectrum. [h] Ground state is uncertain; spectral comparison with py adducts (d_{z^2}) suggests a change of ground state upon py coordination.

Ni–N bond distance of 1.857 (3) Å is in the middle of the 1.81–1.90 Å range for Ni^{II}–N(amidate) bonds in planar complexes.[29,30] Similarly, the Ni–S distance of 2.179 (1) Å is in the normal range of 2.15–2.21 Å for planar Ni^{II} thiolate complexes.[26,28,31] These structural features presumably apply to $[Ni(phma)]^{2-}$ and $[Ni(emi)]^{2-}$. In a purely structural sense, this set of three complexes most closely resembles the planar $Ni^{II}N_2S_2$ complexes Ni(tsalen) (**13**) and Ni(ebmba) (**14**),[31] especially the

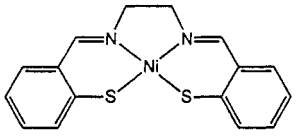

Ni(tsalen) (**13**)

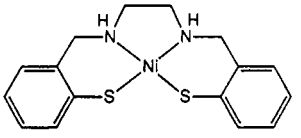

Ni(ebmba) (**14**)

former, for which three Ni–ligand distances are the same as those of $[Ni(ema)]^{2-}$, while one Ni–S distance is 0.04 Å shorter.[31a] As will be seen, their redox properties, however, are very different.

Nickel(III) Complexes. Comparative properties of complexes **5**–**7** described below and other low-potential complexes examined previously are summarized in Table IV.

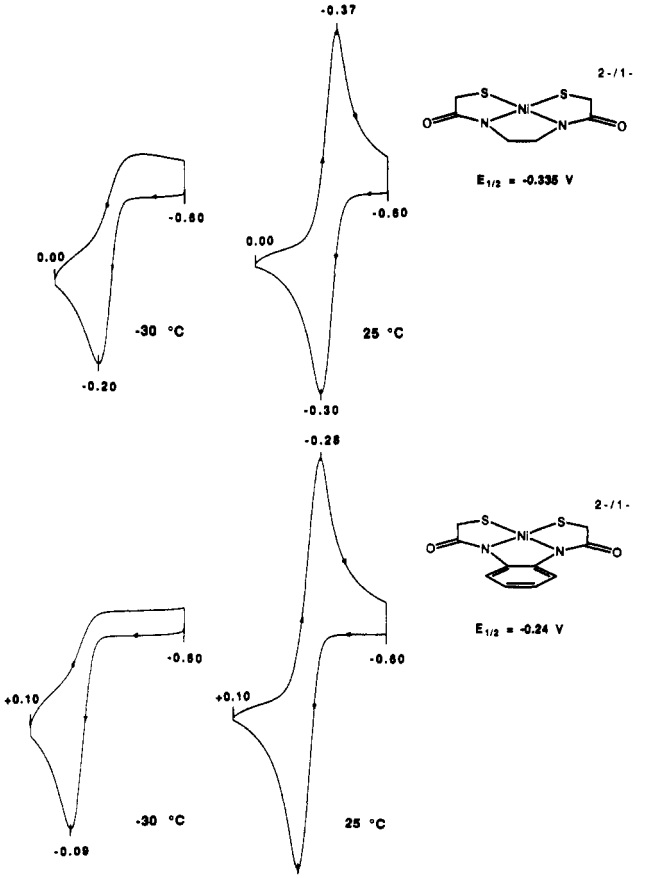

Figure 4. Cyclic voltammograms (20 mV/s) of $[Ni(ema)]^{2-}$ (upper) and $[Ni(phma)]^{2-}$ (lower) at a Pt-foil electrode in DMF solutions at 25 and −30 °C. Peak and half-wave potentials are indicated.

(a) $[Ni(ema)]^-$ and $[Ni(phma)]^-$. The cyclic voltammograms in DMF solutions, shown in Figure 4, reveal electrochemically reversible oxidations of $[Ni(ema)]^{2-}$ and $[Ni(phma)]^{2-}$ at low potentials. Controlled-potential coulometry at room temperature resulted in color changes from red to olive green and gave n = 1.1e^- for each complex. Complete oxidation–reduction cycles over 45–60 min resulted in recovery of only 20% of initial Ni^{II} com-

(30) (a) Lewis, R. M.; Nancollas, G. H.; Coppens, P. *Inorg. Chem.* **1972**, *11*, 1371. (b) Capasso, S.; Mattia, C. A.; Puliti, R.; Zagari, A. *Acta Crystallogr.* **1983**, *C39*, 1517. (c) Stephens, F. S.; Vagg, R. S. *Inorg. Chim. Acta* **1984**, *90*, 17. (d) Kimura, E.; Koike, T.; Nada, H.; Iitaka, Y. *Inorg. Chem.* **1988**, *27*, 1036.

(31) (a) Yamamura, T.; Tadokoro, M.; Kuroda, R. *Chem. Lett.* **1989**, 1245. (b) Yamamura, T.; Tadokoro, M.; Hamaguchi, M.; Kuroda, R. *Chem. Lett.* **1989**, 1481.

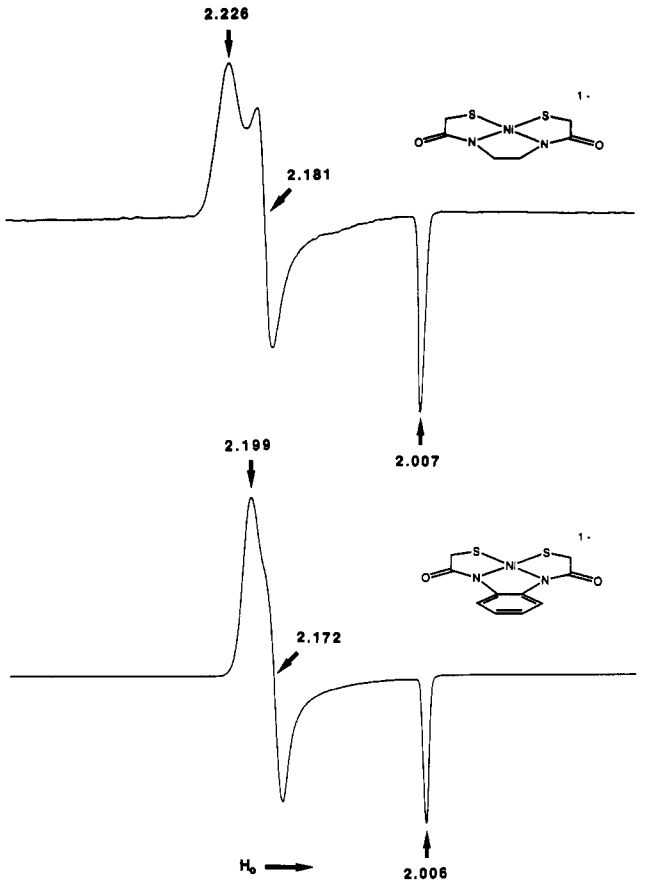

Figure 5. X-Band EPR spectra of electrochemically generated [Ni(ema)]$^-$ and [Ni(phma)]$^-$ in DMF glasses at 100 K. Apparent g values are indicated.

plexes. When the coulometry was performed at −30 °C, n = 0.93e$^-$ for the oxidation of [Ni(ema)]$^{2-}$ and 0.96e$^-$ for [Ni(phma)]$^-$; reduction of the oxidized species at this temperature ceased after passage of 56% and 87%, respectively, of the anodic current. Despite this less than ideal behavior, it can be safely concluded that the oxidation of each Ni^{II} complex is a one-electron process.

The EPR spectra of the electrochemical oxidation products of [Ni(ema)]$^{2-}$ and [Ni(phma)]$^{2-}$ at ambient temperature are shown in Figure 5. The two spectra are nearly axial and have g_{av} = 2.138 and 2.126, respectively. The large anisotropies and $g_{av} \gg 2$ demonstrate the Ni^{III} formulation. Furthermore, $g_\perp > g_\parallel$ and $g_\parallel = 2$ are consistent with a $\sigma^*(d_{x^2})$ ground state.[7]

Cyclic voltammetry at −30 °C resulted in irreversible oxidations (Figure 4), and coulometrically oxidized solutions were EPR-silent. At this temperature, oxidation resulted in an intensification of the red color. When solutions were warmed to room temperature, the EPR spectra of the Ni^{III} complexes were obtained. These results can be reconciled in terms of the coupled reactions shown in (2) (L = ema, phma) involving monomeric and dimeric forms

$$[Ni(L)]^{2-} \underset{+e^-}{\overset{-e^-}{\rightleftharpoons}} [Ni(L)]^- \rightleftharpoons \tfrac{1}{2}[Ni(L)]_2^{2-} \qquad (2)$$

of the Ni^{III} complexes. The dimer is very likely of the lateral type with a Ni(μ-SR)$_2$Ni bridge; its formation is consistent with the usual tendency of tetragonal Ni^{III} species to bind axial ligands.[16e,32] The failure to achieve a coulometric redox cycle with a high degree of recovery of the initial Ni^{II} complexes is doubtless due to the instability of the Ni^{III} species.

(b) [Ni(emi)]$^-$. Of all four-coordinate complexes examined by us, [Ni(emi)]$^{2-}$ is oxidized at the lowest potential and affords the most stable Ni^{III} complex. The cyclic voltammogram in Figure 6 reveals a well-defined oxidation reaction with $E_{1/2}$ = −0.42 V.

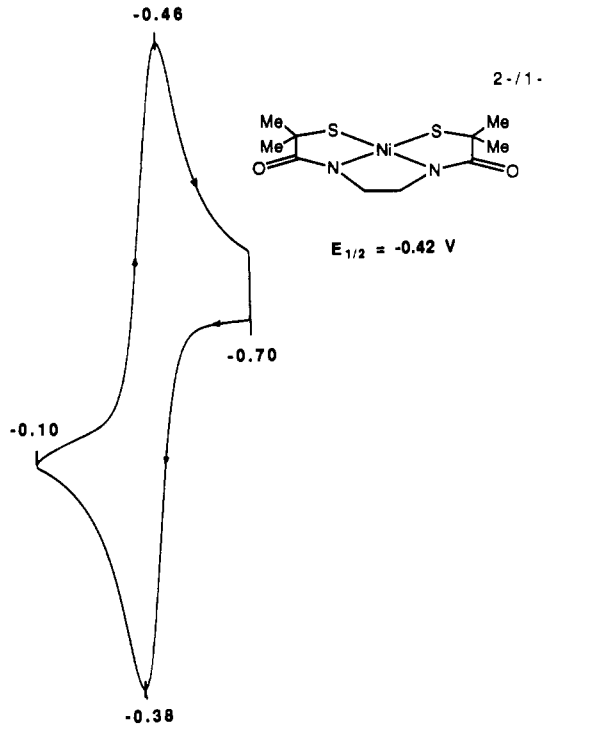

Figure 6. Cyclic voltammogram (20 mV/s) of [Ni(emi)]$^{2-}$ at a Pt-foil electrode in DMF solution at 25 °C. Peak and half-wave potentials are indicated.

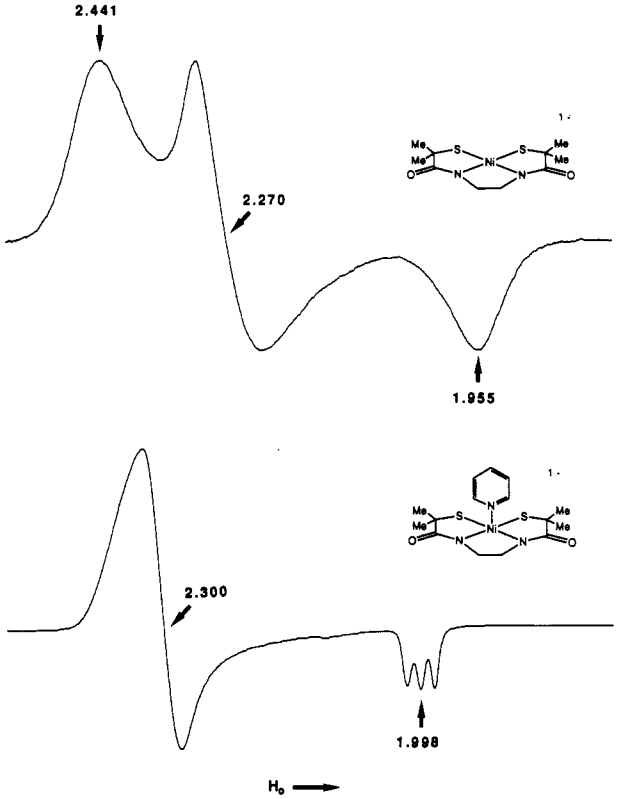

Figure 7. X-Band EPR spectra of electrochemically generated [Ni(emi)]$^-$ in a DMF glass at 25 K and its pyridine adduct [Ni(emi)(py)]$^-$ in a 4:1 DMF/py (v/v) glass at 100 K. Apparent g values are indicated.

During electrolysis at −0.10 V, the color of the solution changes from red to blue-violet. At room temperature and at −30 °C, coulometry gives n = 0.99e$^-$, and an oxidation–reduction cycle can be completed with 80% recovery of the Ni^{II} complex at room temperature and 99% at −30 °C. The oxidation product is characterized by three strong absorption bands at λ_{max} (ϵ_M) 392 (1780), 590 (2200), and 896 nm (4800). When monitored

(32) Zeigerson, E.; Bar, I.; Bernstein, J.; Kirschenbaum, L. J.; Meyerstein, D. *Inorg. Chem.* **1982**, *21*, 73.

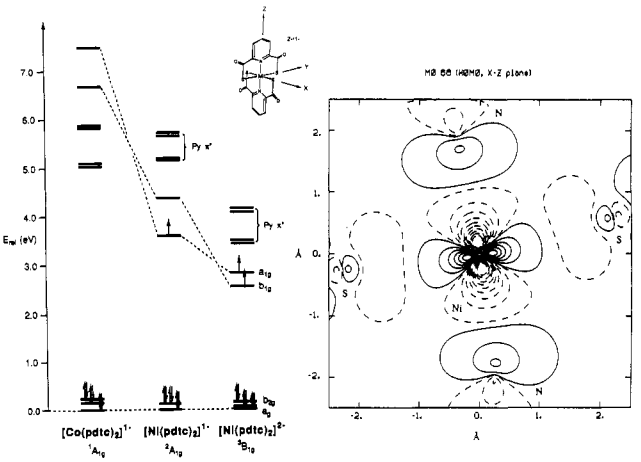

Figure 8. Left: MO energy level diagrams for $[Ni(pdtc)_2]^{2-,-}$ and $[Co(pdtc)_2]^-$ calculated by using the Fenske–Hall method and the indicated coordinate system. Right: plot of the HOMO (a_{1g}, $\sigma^*(d_{z^2})$) of $[Ni(pdtc)_2]^-$, with each successive contour line differing by 0.08 in the value of the wave function.

spectrophotometrically under anaerobic conditions in DMF solution, the extent of decomposition of the oxidized complex within 12 h did not exceed 15%.

No EPR signal for the oxidized complex was observed at 100 K. However, at 25 K the broad rhombic spectrum shown in Figure 7 was obtained. Evidently, the energy separations between ground and excited states is relatively small, leading to extensive spin–orbit mixing of states and a shortened electron spin relaxation time. The spectrum demonstrates that the oxidized species is a Ni^{III} complex. It does not directly convey the ground state because of the significant rhombic splitting of the g values and their unknown relationship to the molecular axis system. The difficulties in deducing ground states of low-spin and low-symmetry d^7 molecules, even in oriented samples, are often considerable and have been treated elsehwere.[33,34] Addition of excess pyridine resulted in an axial spectrum with $g_\perp > g_\parallel$ and a $\sigma^*(d_{z^2})$ ground state. The three ^{14}N hyperfine lines with $a_\parallel^N = 23$ G demonstrate the formation of a monoadduct. The spectrum was observable at 100 K, presumably because binding of an axial donor raises the energy of d_{z^2} and thereby diminishes interactions with excited states. By similar means, the formation of 1:1 adducts with ammonia (g = 2.31, 2.25, 2.01; $a_\parallel^N$ = 24 G), *N*-methylimidazole (g = 2.33, 2.28, 2.00; $a_\parallel^N$ = 25 G), and cyanide (g = 2.21, 2.17, 2.02) was demonstrated.

No evidence was obtained for dimerization of $[Ni(emi)]^-$. This interaction would be sterically impeded by the *gem*-dimethyl groups, which also greatly improve the stability of the complex. Thus far, however, we have not been able to isolate diffraction-quality crystals of $(Et_4N)_2[Ni(emi)]$ or a pure sample of $[Ni(emi)]^-$.

Electronic Structures. Approximate descriptions of the electronic structures of two key pairs of $Ni^{II,III}$ complexes have been sought by using the Fenske–Hall method,[23] which is well suited for examination of comparative electronic structures within the same molecular framework. We have previously shown that in passing from $[Ni(pdtc)_2]^{2-}$ to $[Ni(pdtc)_2]^-$, the mean Ni–S bond distance decreases by 0.14 Å, while the Ni–N distance is nearly unchanged. Further, in going from $[Ni(pdtc)_2]^-$ to $[Co(pdtc)_2]^-$, the M–N distance shortens by 0.09 Å, while the mean M–S distance decreases by only 0.02 Å. These observations constitute part of the proof that the ground state of $[Ni(pdtc)_2]^-$ is $\sigma^*(d_{z^2})$.[13] Calculated orbital energy schemes for the three complexes are shown in Figure 8; orbitals are labeled in idealized D_{4h} symmetry, and the coordinate system is indicated. Actual structures were used in the calculations. Energy orders and orbital compositions are summarized in Table V. For $[Ni(pdtc)_2]^{2-}$ (S = 1), a nearly octahedral orbital energy pattern is found, with the half-filled orbitals in the order $a_{1g} > b_{1g}$. (The splitting between these orbitals (0.4 eV) is not calculated accurately for $S \geq 1$ by this method, which does not include electron spin.) For $[Ni(pdtc)_2]^-$ ($S = {}^1/_2$), the shortened Ni–S bonds lead to the reverse order of the top two orbitals, in agreement with the experimentally determined ground state.[13] Here the HOMO (Figure 8) is mainly $\sigma^*(d_{z^2})$ in nature. For diamagnetic $[Co(pdtc)_2]^-$ the energy order is $a_{1g} > b_{1g} > e_g > b_{2g}$.

Table V. MO Energy Orders and Compositions for Ni(II,III) Complexes

complex	orbitals
$[Ni(pdtc)_2]^{2-}$ [a]	a_{1g} (0.72d_{z^2} + 0.22(N + S) p) > b_{1g}(0.62$d_{x^2-y^2}$ + 0.36S p) > b_{2g}(0.96d_{xy}) > e_g(0.94[d_{xz} + d_{yz}])
$[Ni(pdtc)_2]^-$ [a]	b_{1g}(0.44$d_{x^2-y^2}$ + 0.51S p) > a_{1g}(0.55d_{z^2} + 0.32(N+S) p) ≳ e_g(0.55[d_{xz} + d_{yz}]) > b_{2g}(0.90d_{xy})
$[Ni(nbdt)_2]^{2-}$ [a]	(0.68d_{xy} + 0.29S p) > (0.73d_{yz} + 0.21$d_{x^2-y^2}$) ≳ 0.94d_{xz} > (0.62$d_{x^2-y^2}$ + 0.16d_{z^2} + 0.20d_{yz}) ≈ (0.80d_{z^2} + 0.14$d_{x^2-y^2}$)
$[Ni(nbdt)_2]^-$ [b]	(0.45d_{xy} + 0.48S p) > (0.70d_{xz} + 0.26S p) ≳ (0.61d_{yz} + 0.14$d_{x^2-y^2}$ + 0.20S p) > (0.63$d_{x^2-y^2}$ + 0.14d_{z^2} + 0.15d_{yz}) > (0.79d_{z^2} + 0.14$d_{x^2-y^2}$)

[a] Calculated with actual structure. [b] Assumed structure with Ni–S = 2.07 Å, S–Ni–S = 90°, and C–C–S = 112.7°.

The diamagnetic planar complex $[Ni(nbdt)_2]^{2-}$[14] (**12**) is of considerable interest because of its relationship to $[Ni(pdtc)_2]^{2-,-}$ by removal of two axial ligands, its oxidation to Ni^{III} at a very low redox potential (vide infra), and the compatibility of a $NiS_{3,4}$ coordination unit with EXAFS results.[8] Calculations were performed on the actual structure[14] by using an axis system in which the y axis bisects the chelate ring and the x axis bisects the angle S–Ni–S external to the chelate ring.[35] The LUMO and HOMO are mainly $\sigma^*(d_{xy})$ and $\pi^*(d_{yz} \approx d_{xz})$, respectively, in character, and are separated by 3.7 eV. The four filled orbitals are packed in an interval of 0.16 eV in the energy order in Table V. The structure of $[Ni(nbdt)_2]^-$, which is not known, was modeled in an extensive series of calculations starting from the structure of the Ni^{II} complex in which the Ni–S bond lengths and chelate ring C–C–S bond angles were varied.[35] The LUMO–HOMO order $\sigma^*(d_{xy}) > \pi^*(d_{xz} \approx d_{yz})$ persists over a wide range of parameters. For example, decreasing the Ni–S distance from 2.18 to 2.00 Å with a concomitant change of the C–C–S chelate ring bond angle from 115.4 to 111.3°, at S–Ni–S = 90°, preserves this order. Orbitals calculated for Ni–S = 2.07 Å, the minimal energy configuration along this distortion pathway, are set out in Table V. The LUMO–HOMO gap is large (7.8 eV) relative to the energy interval (0.76 eV) of the four occupied orbitals. The two π^*-type orbitals are nearly degenerate and are separated from the next lowest orbital by 0.57 eV. The greater spread of these four orbitals than in the Ni^{II} case is a reflection of the shorter Ni–S bonds and stronger interactions with ligand orbitals. The

(33) (a) McGarvey, B. R. *Can. J. Chem.* **1975**, *53*, 2498. (b) Nishida, Y.; Kida, S. *Bull. Chem. Soc. Jpn.* **1978**, *51*, 143. (c) Daul, C.; Schläpfer, C. W.; von Zelewsky, A. *Struct. Bonding (Berlin)* **1979**, *36*, 129. In these papers, applications are made to planar and five-coordinate Co^{II} complexes.

(34) If, as seems likely, the progression in rhombicity is $[Ni(phma)]^- < [Ni(ema)]^- < [Ni(emi)]^-$, g_z = 1.955 (Figure 7) and the ground state is approximated as d_{z^2}. In C_2 symmetry $d_{z^2}/d_{x^2-y^2}$ mixing is allowed and values of $g < 2$ are possible.[33] Here the x and y axes lie in the molecular plane and effectively or exactly bisect metal–ligand bond angles.

(35) Because of the nature of the ligand structure of **12**, it was somewhat more convenient to carry out the calculations with an orientation in which the NiS_4 group did not lie precisely in the xy plane. This produces slight mixings of orbitals (Table IV) not permitted in the coplanar arrangement, but the dominant orbital character reamins obvious. In calculations on $[Ni(nbdt)_2]^-$, the structure of the Ni^{II} complex served as the starting point, and its dimensions were then altered to afford structures of D_{2h} microsymmetry. The calculations covered these parameter ranges: Ni–S, 2.00–2.18 Å; S–C–C, 109.1–115.4°; S–Ni–S, 84.7–90.1°. The C–S and C–C distances in the initial structure were held constant. Similar calculations were not pursued at length for NiN_2S_2 complexes because of the larger number of variable structural parameters.

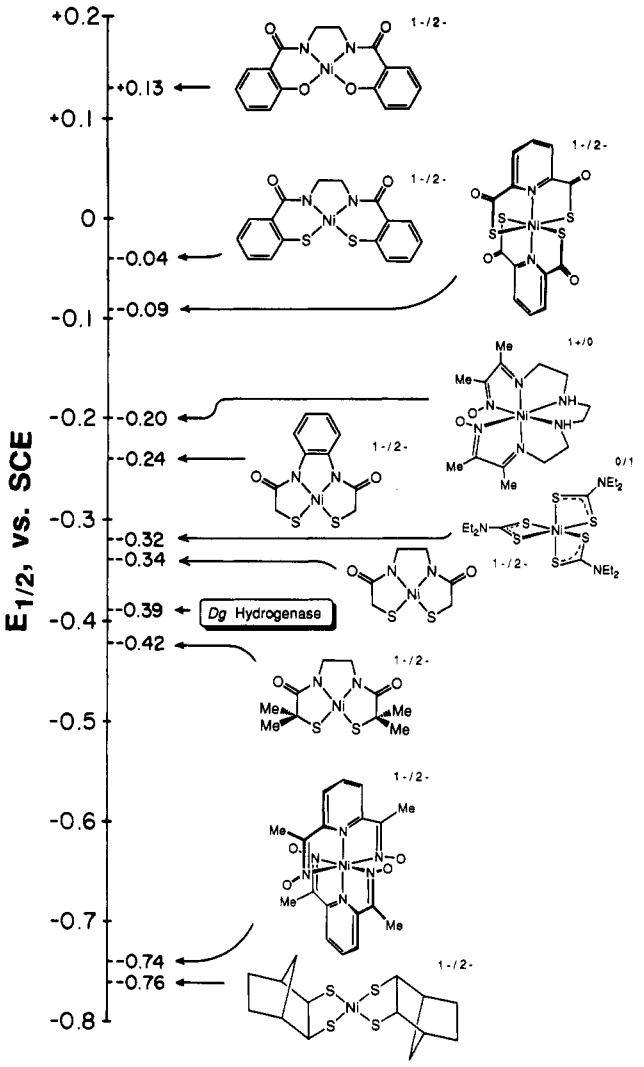

Figure 9. Schematic depiction of low-potential $Ni^{III,II}$ redox couples. Data are taken from this work and other investigations.[4,12-14,39] Data for "high-potential" redox couples are available elsewhere.[7,16a,d,17]

calculations suggest a π^* ground state. Calculations at a higher level for the dithiolene complex $Ni(S_2C_2H_2)_2$[36] predict occupancy of a $\pi^*(d_{yz})$ MO upon reduction to the monoanion. Single-crystal EPR results for $[Ni(mnt)_2]^-$ are entirely consistent with a $\pi^*(d_{yz})$ ground state[37] which, while doubtless more delocalized than is possible for $[Ni(nbdt)_2]^-$, does provide a π^* ground state precedent for a planar d^7 NiS_4 complex.

EPR data for certain oxidized hydrogenases, including that from *D. gigas*,[3,38] are suggestive of a d_{z^2} ground-state configuration. Achievement of this state in the manner of $[Ni(pdtc)_2]^-$, with axial nitrogen ligation, is improbable inasmuch as no ^{14}N hyperfine splittings have been observed with the enzymes. Possible Ni site structures have been considered elsewhere.[13]

Relative Stabilities of Ni^{II} Complexes. The potentials of nearly all low-potential $Ni^{III,II}$ complexes of planar and tetragonal stereochemistry are collected in Table IV. Figure 9 presents a comparative display of these and other low-potential mononuclear complexes,[39,40] which are taken to be those with $E_{1/2} \lesssim +0.1$ V vs SCE in a dipolar aprotic solvent, usually DMF. Here we summarize the leading factors that influence $Ni^{III,II}$ potentials and expand on our earlier discussions[12,13] now that more data are available. Note that all couples in Table IV are comparable in that they involve the same overall charge change (1-/2-) and were examined in the same solvent. Quoted potentials are referenced to the SCE; "reversible" refers to chemically reversible electron transfer on the cyclic voltammetry time scale.

(1) In an overall sense, low potentials are generated by the presence, alone or in combination, of the anionic polarizable ligands of series I (R = alkyl) and the concomitant 1-/2- charge of the

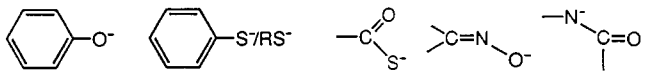

I

redox couple. In the same medium, potentials are lower for couples with the larger negative charges. For the 1+/0, 2+/1+, and 3+/2+ couples, potentials are nearly always >0.5 V,[7] with the 3+/2+ values often in excess of 1 V.[44] Among NiN_2S_2 complexes, for example, neutral **13** and **14** show irreversible oxidations (to unknown products) at +1.0 and +0.35 V,[31b] respectively, whereas dianionic **5**-**7** undergo reversible oxidations at -0.24 to -0.42 V. To series I might also be added alkoxide and oxide, but we lack experimental evidence of their effects on potentials.

(2) The change $2ArO^-$ (**1**) → $2ArS^-$ (**2**) lowers the potential by 170 mV.[45]

(3) The change $2ArS^-$ (**2**) → $2RS^-$ (**5**, R = primary alkyl) lowers the potential by 300 mV, while the change $2RS^-$ → 2 *t*-RS^- (**7**) decreases the potential by 80 mV in the set **2**,**5**,**7** with a constant ethylenediamidinate bridge (but not chelate ring size pattern).

(4) In the pair **5**/**6**, replacement of a 1,2-phenylene with an ethylene bridge stabilizes Ni^{III} by 100 mV, presumably because of the higher basicity of an aliphatic amidate in **5** and a larger extent of electron delocalization in **6**.

(5) The potential difference of 340 mV between **7** and the NiS_4 complex **12** is one measure of the stabilizing effect of thiolate vs amidate. Given the metal-centered nature of the $[Ni(nbdt)_2]^{-,2-}$ couple,[14] it is probable that the $[Ni(edt)_2]^{-,2-}$ couple is similar, in which case its potential (-0.68 V in acetonitrile[26]) indicates an ca. 260 mV stabilization. If the comparison is widened to the simplest dithiolene complexes ($[Ni(S_2C_2H_2)_2]^{-,2-}$[43b]), the apparent stabilization is 420 mV.

(6) Although somewhat imprecise comparisons, the results in (5) together with the 650-mV potential difference between **3** and **4** indicate that, of the ligands in series I, alkanethiolate and oximate are the most effective in stabilizing Ni^{III}.

In the foregoing, aspects 2 and 3 appear to derive from changes in basicity, the more basic ligand preferentially stabilizing Ni^{III}.

(36) Herman, Z. S.; Kirchner, R. F.; Loew, G. H.; Mueller-Westerhoff, U. T.; Nazzai, A.; Zerner, M. C. *Inorg. Chem.* **1982**, *21*, 46.
(37) Maki, A. H.; Edelstein, N.; Davison, A.; Holm, R. H. *J. Am. Chem. Soc.* **1964**, *86*, 4580. mnt = maleonitriledithiolate(2-).
(38) Teixeira, M.; Fauque, G.; Moura, I.; Lespinat, P. A.; Berlier, Y.; Prickril, B.; Peck, H. D., Jr.; Xavier, A. V.; LeGall, J.; Moura, J. J. G. *Eur. J. Biochem.* **1987**, *167*, 47.
(39) (a) Couple at -0.20 V: Chakravorty, A. *Isr. J. Chem.* **1985**, *25*, 99. (b) Couple at -0.32 V: Lachenal, D. *Inorg. Nucl. Chem. Lett.* **1975**, *11*, 101. Hendrickson, A. R.; Martin, R. L.; Rohde, N. M. *Inorg. Chem.* **1975**, *14*, 2980.
(40) There are several exclusions from Table IV and Figure 9: (i) Ni^{II} tetraazamacrocycles for which it is not clear that the oxidation reactions are metal-centered;[41] (ii) the nonphysiological and otherwise rather special cases of Cp and carborane Ni complexes;[42] (iii) Ni dithiolenes,[43] $[Ni(S_2C_2R_2)_2]^{-,2-}$ and related complexes, for which the Ni^{II} description is adequate for the 2- state, in which the ligand is an ene dithiolate. But the Ni^{III} formulation for the 1- state is oversimplified because of the extensive delocalization of the odd electron which, however, has some d-orbital character.[37]
(41) Busch, D. H. *Acc. Chem. Res.* **1978**, *11*, 392.
(42) (a) Wilson, R. J.; Warren, L. F., Jr.; Hawthorne, M. F. *J. Am. Chem. Soc.* **1969**, *91*, 758. (b) Warren, L. F., Jr.; Hawthorne, M. F. *J. Am. Chem. Soc.* **1970**, *92*, 1157. (c) Rietz, R. R.; Dustin, D. F.; Hawthorne, M. F. *Inorg. Chem.* **1974**, *13*, 1580.
(43) (a) McCleverty, J. A. In *Reactions of Molecules at Electrodes*; Hush, N. S., Ed.; Wiley-Interscience: New York, 1971; pp 403-492. (b) Hoyer, E.; Dietzsch, W.; Hennig, H.; Schroth, W. *Chem. Ber.* **1969**, *102*, 603.
(44) It might be noted that the $[Ni(OH_2)_6]^{3+,2+}$ potential has been estimated to be 2.26 V!: Bhattacharya, S.; Mukherjee, R.; Chakravorty, A. *Inorg. Chem.* **1986**, *25*, 3448.
(45) Stabilization of Ni^{III} by O → S replacement has been observed previously for octahedral complexes, but the effect could not be expressed as a potential difference owing to the irreversibility of certain redox reactions: Ray, D.; Pal, S.; Chakravorty, A. *Inorg. Chem.* **1986**, *25*, 2674.

Perhaps throughout, but most probably for Ni^{II} complexes **5–7**, tight-fitting ligands promote the relative stability of Ni^{III}.[46]

This investigation, together with others directed toward an interpretation of Ni potentials in hydrogenases,[11a,12-14] has been successful in producing metal-centered redox couples of heretofore unattained low potentials. When nominally compared (Figure 9), three couples have lower potentials than *D. gigas* hydrogenase, in which the environment around the Ni site is unknown. The pH dependence of the enzyme potential, determined at pH 7.2–8.5,[4] is consistent with the proton-coupled electron-transfer reaction (3). In this event, the potential of the pH-independent

$$[Ni^{III}L_n]^z + H^+ + e \rightleftharpoons [Ni^{II}L_nH]^{z-1} \quad (3)$$

electron transfer must be less than ca. −0.46 V. This estimate is very close to the potential of $[Ni(nbdt)_2]^{-,2-}$ in methanol (−0.46 V),[14] which may be taken to approximate the effect of protic solvent and hydrogen bonding on the potential of a protein-bound $[Ni(SR)_4]^{-,2-}$ couple. If a "correction" of 300 mV is applied to the potentials of Table V, only oximate complex **4** and thiolate complex **12** have potentials near that of the enzyme. While the comparisons are obviously inexact, the fact is that no synthetic Ni redox couple with ligand type(s) of known occurrence in proteins except $[Ni(nbdt)_2]^{-,2-}$ comes close to the estimated potential of the Ni site in *D. gigas* hydrogenase. The effect of hydrogen bonding by protic solvents or protein structure is preferentially to stabilize the reduced member of a redox couple; there are other well-documented examples of this effect.[13,47] Note the highly positive potentials of the glycyl peptide complexes **15–18** in aqueous solution.[16a]

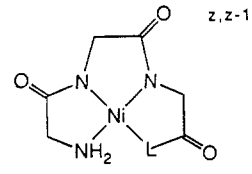

	L	z	E^0, V
15	O	0	0.61
16	NH	0	0.59
17	$NCH_2CO_2^-$	1-	0.55
18	NCH_2CONH_2	0	0.60

This group includes one 1−/2− couple, $[Ni^{III,II}(H_{-3}G_4)]^{-,2-}$ (**17**), with three amidate nitrogen binding sites. Even in 50% water/acetonitrile (v/v) the potential of **16** is unchanged,[16d] indicating that strong hydrogen-bonding interactions are little disturbed.

We conclude that cysteinate is the most effective native ligand in stabilizing Ni^{III} but caution that not all biological modes of metal ligation may have been discovered[15] and that we do not know what, if any, structural changes attend the redox reaction of the protein-bound site. It would appear that entry to the catalytic cycle of hydrogenase from a resting low-potential Ni^{II} state requires protonation at or near the Ni site in order to raise the potential for reduction, resulting in the generation of Ni^{I} (assuming its involvement[1-3]) or possibly Ni^{III}–H^-, to an accessible value. If NiS_4-type species are considered, the potential of the $[Ni^{II,I}(mnt)_2]^{2-,3-}$ couple in acetonitrile is very negative (−1.7 V[48]), and this is a favorable case owing to the presence of cyano groups on the chelate rings. With the exposure of those ligand factors which promote low $Ni^{III,II}$ potentials of structurally invariant redox couples, as revealed in Table IV and Figure 9, the next step is to develop analogue reaction systems with hydrogenase activity. Such experiments are underway.

Acknowledgment. This research was supported by NSF Grant CHE 89-03283. X-ray diffraction equipment was obtained through NIH Grant 1 S10 RR 02247. We thank Dr. C. Campana of Siemens Analytical X-Ray Instruments, Inc., for collection of X-ray data.

Supplementary Material Available: For $(Et_4N)_2[Ni(ema)]\cdot 2H_2O$, tables of intensity collection and crystal data, interatomic distances and angles, atom positional parameters, anisotropic temperature factors, and calculated hydrogen atom positions (5 pages); a listing of calculated and observed structure factors (13 pages). Ordering information is given on any current masthead page.

(46) Other than for **3**, where Ni^{II} and Ni^{III} structures are known, we have insufficient structural information to evaluate this point. The data for **3** indicate a 0.14 Å smaller effective radius for Ni^{III} in the equatorial plane than for octahedral Ni^{II}, and Shannon radii suggest a 0.07 Å smaller radius for Ni^{III} in low-spin complexes (Shannon, R. D. *Acta Crystallogr.* **1976**, *A32*, 751). Note that the NiS_4 portion of $[Ni(nbdt)_2]^{2-}$ is square-planar and that the complex suffers from no evident steric destabilization. If so, this reinforces the intrinsic effectiveness of thiolate as a ligand for producing low-potential metal-centered redox couples.

(47) (a) Hill, C. L.; Renaud, J.; Holm, R. H.; Mortenson, L. E. *J. Am. Chem. Soc.* **1977**, *99*, 2549. (b) Mascharak, P. K. *Inorg. Chem.* **1986**, *25*, 246. (c) Holm, R. H.; Ciurli, S.; Weigel, J. A. *Prog. Inorg. Chem.* **1990**, *38*, 1 (see also references therein).

(48) Geiger, W. E., Jr.; Mines, T. E.; Senftleber, F. C. *Inorg. Chem.* **1975**, *14*, 2141 (mnt = maleonitriledithiolate(2−)).